*Proc SPIE **5582**, Advanced Optoelectronics and Lasers, p154-161 (2004) – copy of text*

EXACT ANALYTICAL HELMHOLTZ BRIGHT AND DARK SOLITONS

P. Chamorro-Posada[1], G.S. McDonald[2]

[1]*Departamento de Teoría de la Señal y Comunicaciones e Ingeniería Telemática*
Universidad de Valladolid, ETSI Telecomunicación, Campus Miguel Delibes s/n
47011 Valladolid, Spain
Phone: +34 983 185545, Fax: +34 983 423667, e-mail: pedcha@tel.uva.es
[2]*Joule Physics Laboratory, School of Sciences, Institute of Materials Research*
University of Salford, Salford M5 4WT, UK
Phone: +44 161 295 5079, Fax: +44 161 295 5147, e-mail: g.s.mcdonald@salford.ac.uk

INTRODUCTION

Spatial optical solitons play a fundamental role in the dynamics of nonlinear beams [1] and an accurate description of aspects such as oblique propagation and mutual interactions is essential. Solitons that propagate at modest or large angles relative to the reference longitudinal direction, or to each other, experience a type of non-paraxiality that can be accurately described by a nonlinear Helmholtz equation (NHE). Considering a single soliton beam that coincides with the longitudinal axis ζ, off-axis propagation results if only the axis is rotated, whereby $\partial_{\zeta\zeta}$ is no longer negligible. Moreover, the resulting NHE can describe the total electric field of both forward and backward propagating components, and thus soliton interactions at *arbitrary* angles.

Some optical contexts, such as intense self-focusing, give rise to a more general type of nonparaxiality [2-4]. Paraxiality is commonly defined through a small parameter $\kappa = w_0^{\,2} / 4L_D^{\,2}$, where w_0 is beam width, $L_D = kw_0^{\,2}/2$ and $k = n_0\omega/c$. Order of magnitude analysis [2,3], based on κ, then yields leading correction terms to a paraxial wave equation. A near-paraxial beam, well-described by scalar electric field and refractive index distributions, if considered in a reference frame rotated by θ, acquires an effective transverse velocity V, but the beam itself remains intrinsically scalar in character. The usual paraxial condition, $\kappa \approx 0$, is still preserved but now $2\kappa V^2 = \tan^2\theta$ can assume arbitrarily large values. The presence of this type of, potentially dominant, non-paraxial correction is demonstrated through exact solution of the NHE. Helmholtz-type nonparaxiality, alone, is thus shown to result in non-trivial modifications to soliton propagation characteristics.

HELMHOLTZ BRIGHT SOLITONS

The equivalence of the nonparaxial nonlinear Schrödinger equation (NNLS) and the appropriate NHE has recently been noted [5]. This permits identification of nonparaxial generalizations of conventional soliton theory as exact analytical Helmholtz *bright* soliton solutions [6]. Physical interpretations [6] and analytical properties [7] of Helmholtz bright solitons have been presented and allowed the development and testing of new nonparaxial beam propagation techniques [8]. To highlight the modifications to paraxial theory, here we solve the equivalent *focusing* NNLS [5-8]:

$$\kappa\frac{\partial^2 u}{\partial\zeta^2} + i\frac{\partial u}{\partial\zeta} + \frac{1}{2}\frac{\partial^2 u}{\partial\xi^2} + |u|^2 u = 0 \qquad (1)$$

where $\zeta = z/L_D$, $\xi = \sqrt{2}x/w_0$ and $u(\xi,\zeta) = \left(k|n_2|L_D/n_0\right)^{1/2} B(\xi,\zeta)$ are longitudinal and transverse coordinates and field amplitude, respectively, in terms of the Kerr coefficient n_2, unscaled variables z, x and the field envelope B defined by $E(x,z) = B(x,z)\exp(ikz)$. We find the following general Helmholtz bright soliton:

$$u(\xi,\zeta) = \eta \operatorname{sech}\left[\frac{\eta(\xi + V\zeta)}{\sqrt{1+2\kappa V^2}}\right] \exp\left[i\left(\frac{1+2\kappa\eta^2}{1+2\kappa V^2}\right)^{1/2}\left(-V\xi + \frac{\zeta}{2\kappa}\right)\right] \exp\left(\frac{-i\zeta}{2\kappa}\right) \tag{2}$$

where η, V and κ are the amplitude, transverse velocity and nonparaxial parameters, respectively. When nonparaxial effects are negligible, i.e. when $\kappa \to 0$, $\kappa\eta^2 \to 0$ and $\kappa V^2 \to 0$, one recovers the well-known paraxial soliton solution of the nonlinear Schrödinger equation (NLS):

$$u(\xi,\zeta) = \eta \operatorname{sech}[\eta(\xi + V\zeta)] \exp\left[-iV\xi + \frac{i}{2}\left(\eta^2 - V^2\right)\zeta\right]. \tag{3}$$

The width of the Helmholtz bright soliton is given by $\xi_0 = \left(1+2\kappa V^2\right)^{1/2}/\eta$. The soliton's area is thus proportional to $\xi_0\eta = \left(1+2\kappa V^2\right)^{1/2}$ and depends on both the transverse velocity and the actual size of the beam (through κ). The latter property reflects the fact that the solutions of the NNLS are invariant under transformations:

$$\xi = \frac{\xi' + V\zeta'}{\left(1+2\kappa V^2\right)^{1/2}}, \quad \zeta = \frac{-2\kappa V\xi' + \zeta'}{\left(1+2\kappa V^2\right)^{1/2}} \tag{4}$$

$$u(\xi,\zeta) = \exp\left\{i\left[\frac{V\xi'}{\left(1+2\kappa V^2\right)^{1/2}} + \frac{1}{2\kappa}\left(1 - \frac{1}{\left(1+2\kappa V^2\right)^{1/2}}\right)\zeta'\right]\right\} u'(\xi',\zeta'), \tag{5}$$

from which the well-known Galilean transformation invariance of the NLS is recovered in the appropriate paraxial limit. The transformations (4)-(5) correspond to a rotation of the solution in the original (unscaled) coordinate system by an angle θ, given by $\sec\theta = \left(1+2\kappa V^2\right)^{1/2}$; this allows the analysis to be extended to common nonparaxial situations in which off-axis soliton beams are considered. We now demonstrate that these transformations can be used to predict the long-term evolution of Helmholtz bright soliton when they are used in conjunction with analytical paraxial techniques.

Numerical studies are needed to address important questions regarding the stability of nonlinear solutions and whether they can be generated from arbitrary initial conditions. Our exact Helmholtz solutions, and properties of the NHE, have provided a framework for testing existing nonparaxial beam propagation methods. Indeed, distinct methods were found to yield quantitatively different results and we found it necessary to derive new algorithms [8]. Here, we consider Helmholtz bright soliton formation from the initial condition $u(\xi,0) = \operatorname{sech}(\xi)\exp(-iS_0\xi)$, which corresponds to an exact paraxial soliton with $\eta = 1$ and $V = S_0$. Figure 1 shows the evolution of the beam area for $\kappa = 10^{-3}$ and three different values of S_0 (giving propagation angles of $\theta = 12.9°, 26.6°$ and $42.1°$). The initial value problems can be shown to be equivalent to those involving perturbed paraxial solitons with $V = 0$ (their widths having been reduced by factors of $\left(1+2\kappa V^2\right)^{1/2}$). Thus, the long term evolution of the soliton beams can be predicted using inverse scattering techniques. Horizontal lines display the long term evolution values predicted from such analysis. It can be seen that the beam parameters undergo decaying oscillations towards their predicted asymptotic values.

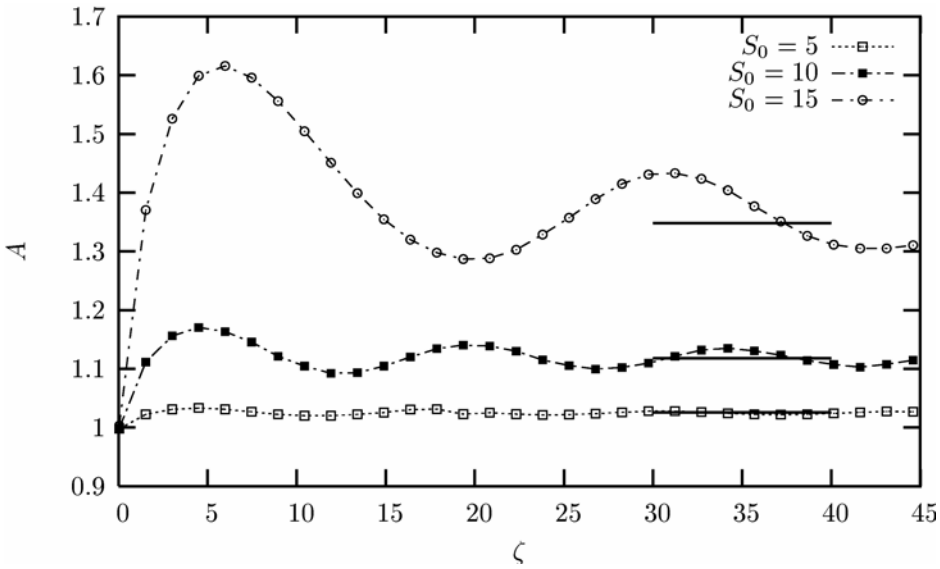

Fig. 1 - Formation of Helmholtz bright solitons from paraxial soliton initial conditions. The evolution of the beam area is plotted for profiles launched at three distinct input angles.

These simulations demonstrate the inappropriateness of paraxial soliton solutions in oblique beam propagation and that the Helmholtz solutions are both stable and act as attractors in nonlinear beam evolution.

HELMHOLTZ DARK SOLITONS

Now, we present the general Helmholtz *dark* soliton solution for a defocusing Kerr nonlinearity. Again, to highlight the modifications to paraxial theory, we solve the equivalent *defocusing* NNLS:

$$\kappa\frac{\partial^2 u}{\partial\zeta^2}+i\frac{\partial u}{\partial\zeta}+\frac{1}{2}\frac{\partial^2 u}{\partial\xi^2}-|u|^2 u=0 \tag{6}$$

For simplicity, a uniform background field u_0 is assumed. A general dark solution of Eq. (6) is then found to be [9]

$$u(\xi,\zeta)=u_0\left(A\tanh\Theta+iF\right)\exp\left[i\left(\frac{1-4\kappa u_0{}^2}{1+2\kappa V^2}\right)^{1/2}\left(-V\xi+\frac{\zeta}{2\kappa}\right)\right]\exp\left(-i\frac{\zeta}{2\kappa}\right), \tag{7}$$

where

$$\Theta=\frac{u_0 A(\xi+W\zeta)}{\left(1+2\kappa W^2\right)^{1/2}} \tag{8}$$

and

$$W=\frac{V-V_0}{1+2\kappa V V_0} \tag{9}$$

is a net transverse velocity involving V (from choice of reference direction) and V_0 (a grey soliton component), given by

$$V_0=\frac{u_0 F}{\left[1-\left(2+F^2\right)2\kappa u_0{}^2\right]^{1/2}}. \tag{10}$$

F and A are real constants, with $F = \pm\left(1 - A^2\right)^{1/2}$. $F = 0$ corresponds to Helmholtz black solitons, while $|F| > 0$ yields grey solitons. In the paraxial limit, the NLS dark soliton is obtained:

$$u(\xi,\zeta) = u_0\left(A\tanh\Theta + iF\right)\exp\left(-iV\xi\right)\exp\left(-iu_0{}^2\zeta - i\frac{1}{2}V^2\zeta\right), \tag{11}$$

where

$$\Theta = u_0 A\left[\xi + \left(V - Fu_0\right)\zeta\right]. \tag{12}$$

Non-zero W corresponds to off-axis propagation. Geometrical considerations then imply that the beam width projected onto the transverse axis should increase (a feature absent from paraxial theory). In fact, the inverse dark soliton width is given by:

$$\xi_0^{-1} = \frac{u_0 A}{\left(1 + 2\kappa W^2\right)^{1/2}}. \tag{13}$$

The beam width enlargement factor can also be written as $\left(1 + 2\kappa W^2\right)^{1/2} = \sec\left(\theta - \theta_0\right)$, where $\theta_0 = \sec^{-1}\left[\left(1 + 2\kappa V_0{}^2\right)^{1/2}\right]$ is the angle associated with V_0 and $\theta = \sec^{-1}\left[\left(1 + 2\kappa V^2\right)^{1/2}\right]$ is defined by choice of reference frame.

To explore whether Helmholtz dark solitons are spontaneously created from an initial field profile that does not correspond to an exact soliton, we consider the initial condition $u(\xi,0) = u_0\tanh\left(u_0\xi\right)\exp\left(-iS_0\xi\right)$. In a paraxial framework, a single black soliton results with transverse velocity S_0. For $\kappa u_0{}^2 << 1$, the NHE evolution can be shown to be equivalent to the propagation of an initially perturbed (reduced width) on-axis NLS black soliton. Paraxial techniques then verify that one expects the generation of only one Helmholtz soliton. Figure 2 shows the evolving beam widths for u_0=1, κ=10^{-3} and three different values of S_0 corresponding to propagation angles of $\theta = \tan^{-1}\left(\sqrt{2\kappa}V\right)$ = 12.9º, 26.6º and 42.1º, respectively.

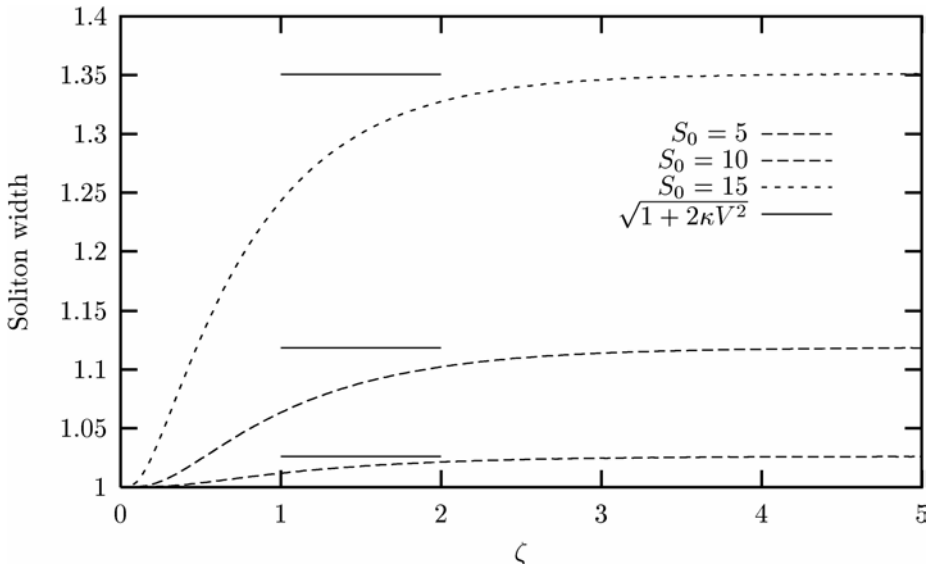

Fig. 2 - Evolution of beam widths for initially perturbed off-axis Helmholtz black solitons (horizontal lines denote analytical predictions for their asymptotic values).

The predicted asymptotic values of the Helmholtz beam width are given by $\left(1+2\kappa V^2\right)^{1/2}$ where $V = S_0/\left(1-2\kappa S_0{}^2\right)^{1/2}$ when $\kappa u_0{}^2 << 1$. While similarly perturbed Helmholtz bright solitons undergo large oscillations over long propagation distances, dark beams are found to exhibit a surprisingly fast convergence to the asymptotic solutions.

COHERENT HELMOLTZ SOLITON COLLISIONS

The interactions of optical spatial solitons in various types of media have been extensively studied both theoretically and experimentally. Three fundamental interaction geometries can be identified: almost exactly copropagating solitons, almost exactly counterpropagating solitons and collisions at intermediate angles. At small interaction angles (close to exact copropagation), the spatial problem is fully analogous to the interaction of temporal solitons in optical fibres. This thus corresponds to a paraxial geometry where accurate analytical and numerical results can be derived from the NLS [10,11]. The other extreme, of near exact counterpropagation of beams, has also been studied using the paraxial approximation [12,13]. Models consisting of coupled equations for the forward and backward beams have been employed, rendering calculation of the numerical solution more involved. However, modeling the interaction of spatial solitons at any angle ranging between these two extremes requires accounting for Helmholtz-type nonparaxiality. Various contexts and proposed photonic devices [14-16] involve multiplexed solitons at such intermediate angles where, for example, interaction trajectory phase shifts need to be accurately described. Paraxial theory can also be shown to be inconsistent, as it fails to uniquely define soliton propagation angles in the laboratory frame. To date, intermediate angle configurations have only been analysed using NLS theory. In this section, we present the first detailed account of the interaction properties of coherent Helmholtz bright solitons in a nonlinear Kerr medium. A physically consistent picture emerges that yields results that differ substantially from predictions derived from the paraxial NLS.

The NHE can accurately capture the behaviour of multiple soliton beams that simultaneously propagate at arbitrary angles (including counterpropagation geometries). Here, we consider two such beams, $u_1(\xi,\zeta)$ and $u_2(\xi,\zeta)$, propagating at angles θ and $-\theta$ to the z-axis, respectively, and set $u(\xi,\zeta) = u_1(\xi,\zeta) + u_2(\xi,\zeta)$ in (1). The simultaneous presence of the beams modulates the refractive index of the Kerr medium according to $|u|^2 = |u_1|^2 + |u_2|^2 + u_1 u_2^* + u_2 u_1^*$. The last two terms define a (real) holographic grating [17] that is superimposed on variations due to the individual intensities of the solitons. Three distinct effects then arise from the nonlinearity $|u|^2 u$: a term proportional to the jth beam amplitude u_j and its intensity $|u_j|^2$, accounting for self-phase modulation, a term of the form $2|u_{3-j}|^2 u_j$, corresponding to cross-phase modulation (XPM) of the interacting beams, and phase-sensitive terms proportional to $u_j^2 u_{3-j}^*$. The index grating is absent from interactions of incoherent solitons, whereby there are no holographic terms and the XPM term is reduced to $|u_{3-j}|^2 u_j$. To describe the full range of coherence, one introduces a grating factor h and expresses the total XPM contribution as $(1+h)|u_{3-j}|^2 u_j$, which has limits: $h = 0$ for incoherent interactions, and $h = 1$ for coherent interactions.

For small interaction angles, the phase-sensitive terms contribute notably to the collision process, and result in phenomena that are strongly dependent on relative soliton phase. The terms are important when they generate field components with wavevectors that are resonant with the interacting beams. As the interaction angle increases, the phase-sensitive terms be-

come non-resonant and can be neglected in the analysis. Within a full NHE description, or that given by the NLS, their effect is to produce new spectral components in the interaction region that are reabsorbed by the propagating solitons after their collision [18]. NHE-governed evolution of two interacting beams then reduces to two-coupled equations:

$$\kappa \frac{\partial^2 u_j}{\partial \zeta^2} + i \frac{\partial u_j}{\partial \zeta} + \frac{1}{2} \frac{\partial^2 u_j}{\partial \xi^2} + \left[|u_j|^2 + (1+h)|u_{3-j}|^2 \right] u_j = 0 \tag{14}$$

whereby collision effects can be understood in terms of respective beam intensities. An important parameter in the collision process is the trajectory phase shift of the solitons. We denote this as Δ and define its meaning in Figure 3. It is important to note that, in a paraxial description, Δ goes monotonically to zero as the interaction angle increases [18].

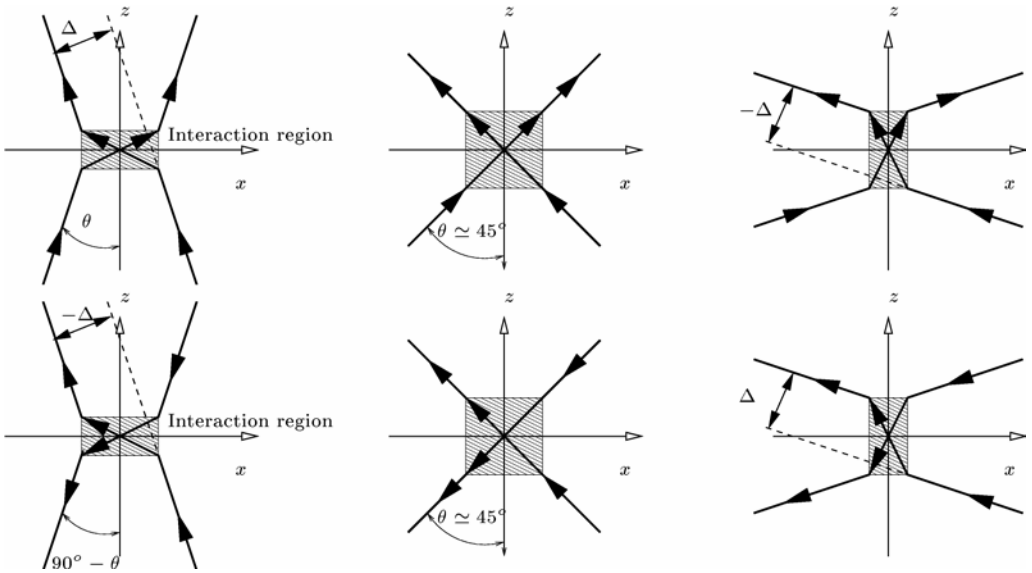

Fig. 3 - Geometry of Helmholtz soliton collisions in which interactions are dominated by the individual beam intensities. Top panel: copropagating solitons; bottom panel: counterpropagating solitons.

Figure 3 shows the geometry of Helmholtz soliton collisions in the absence of phase-sensitive terms in the evolution equations; a clear symmetry arises in the problem when the interaction is dominated by the intensities of the beams. In the configurations of copropagating solitons shown in the top panel, the two input beams propagate at angles of θ and $-\theta$ to the z axis, respectively. For large interaction angles, the collision geometry has similar symmetry to that of small propagation angles, except that Δ has to change sign as θ crosses the value of 45^o (it is precisely zero at this angle). Each configuration of copropagating interaction can be rotated by 90^o to give a corresponding description of counterpropagating interaction (shown in the bottom panel). For example, the case shown leftmost in the bottom panel corresponds to the configuration of the rightmost plot in the top panel. Identification of such symmetry permits an alternative approach to the numerical simulation of large angle interactions, where numerical problems can otherwise arise. Since the NHE solution can support both forward and backward components, a boundary condition for numerical integration may contain an input soliton (propagating in the forward direction) along with an output soliton (that has resulted from propagation in the backward direction). Thus, if a collision involves negligible radiation (which is generally true, other than for cases of near exact counterpropagation [13]), one can obtain a valid counterpropagating solution by rotating the copropagating solution by 90 degrees.

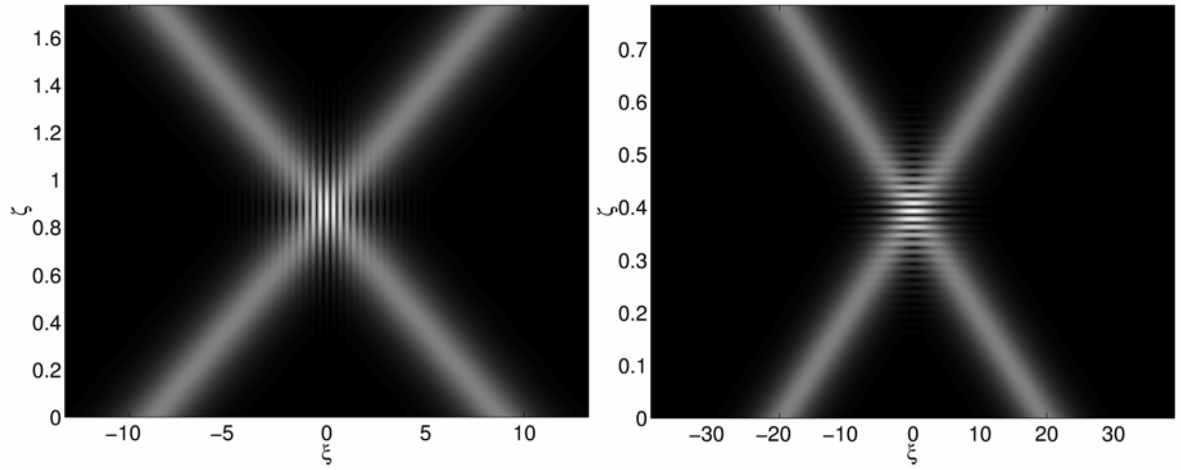

Fig. 4 – Intensity profiles of two interacting solitons with equal amplitudes. Left panel: two co-propagating solitons; right panel: two counterpropagating solitons.

In figure 4, we map the total field intensity for two interacting Helmholtz solitons in copropagation and counterpropagation configurations; the index grating induced in the medium occurs in the transverse and longitudinal directions, respectively. In both cases $\kappa = 10^{-3}$, while $V = 10$ in the copropagation case (left panel) and $V = 50$ in the counterpropagation case (right panel). Both configurations correspond to approximately the same angle (θ=24.095° and 90°-θ=24.095°, respectively).

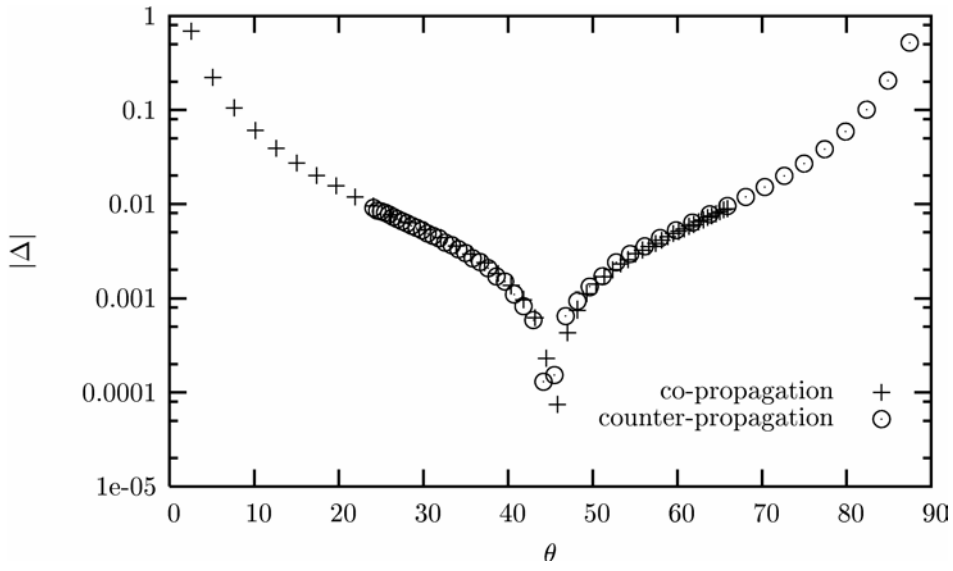

Fig. 5 - Magnitude of the trajectory phase shift, as defined in Fig. 3, as a function of interaction angle θ for both copropagation and counterpropagation configurations (κ=10^{-3}).

Figure 5 shows the magnitude of the trajectory phase shift, as a function of θ, for both copropagation and counterpropagation initial conditions. The value of Δ is obtained by fitting the numerical data to a pair of hyperbolic secant functions, before and after each collision, to estimate soliton positions as a function of ζ. The trajectory phase shift is then derived from the soliton shift in the ξ direction, Δ_ξ, using $\Delta=\Delta_\xi \cos\theta$, where $\cos\theta = 1/\sqrt{1+2\kappa V^2}$.

CONCLUSIONS

In this paper, we have presented exact analytical Helmholtz bright and dark soliton solutions for a Kerr nonlinearity. Simulations verify that these solutions are both robust and act as attractors in nonlinear beam dynamics. Results dealing with the coherent interaction of Helmholtz bright solitons have also been presented, for the first time. These considerations extend previous (paraxial) studies that are only valid for vanishingly small interaction angles.

REFERENCES

1. G. I. Stegeman and M. Segev, "Optical spatial solitons and their interactions: Universal ity and diversity," *Science*, vol 286, p. 1518, 1999.
2. S. Chi and Q. Guo, "Vector theory of self-focusing of an optical beam in Kerr media," *Opt. Lett.*, vol. 20, p. 1598, 1995.
3. A. Ciattoni, P. Di Porto, B. Crosignani and A. Yariv, "Vectorial nonparaxial propagation equation in the presence of a tensorial refractive-index perturbation," *J. Opt. Soc. Am. B*, vol. 17, p. 809, 2000.
4. S. Blair, "Nonparaxial one-dimensional spatial solitons," *Chaos*, vol. 10, p. 570, 2000.
5. P. Chamorro-Posada, G. S. McDonald and G. H. C. New, "Exact soliton solutions of the nonlinear Helmholtz equation: communication," *J. Opt. Soc. Am. B*, vol. 19, p. 1216, 2002.
6. P. Chamorro-Posada, G. S. McDonald and G. H. C. New, "Nonparaxial solitons," *J. Mod. Opt.,* vol. 45, p. 1111, 1998.
7. P. Chamorro-Posada, G. S. McDonald and G. H. C. New, "Propagation properties of nonparaxial spatial solitons," *J. Mod. Opt.,* vol. 47, p. 1877, 2000.
8. P. Chamorro-Posada, G. S. McDonald and G. H. C. New, "Nonparaxial beam propaga tion methods," *Opt. Commun.,* vol. 19, p. 1, 2001.
9. P. Chamorro-Posada and G. S. McDonald, "Helmholtz dark solitons," *Opt. Lett.,* vol. 28, p. 825, 2003.
10. J. P. Gordon, "Interaction forces among solitons in optical fibers," *Opt. Lett*., vol. 8, p. 596, 1983.
11. R. Hirota, "Exact envelope-soliton solutions of a nonlinear wave equation," *J. Math. Phys.*, vol. 14, p. 805, 1973.
12. M. Haelterman, A. P. Sheppard and A. W. Snyder, "Bimodal counterpropagating spatial solitary-waves," *Opt. Commun*., vol. 103, p. 145, 1993.
13. O. Cohen, R. Uzdin, T. Carmon, J. W. Fleischer, M. Segev and S. Pdouov, "Collisions between optical spatial solitons propagating in opposite directions," *Phys. Rev. Lett*., vol. 89, art. no. 229901, 2002.
14. P. D. Miller and N. N. Akhmediev, "Transfer matrices for multiport devices made from solitons," *Phys. Rev. E*, vol. 53, p. 4098, 1996.
15. H. T. Tran, R. A. Sammut and W. Samir, "Interaction of self-guided beams of different frequencies," *Opt. Lett*., vol. 19, p. 945, 1994.
16. F. Chiarluce, E. Gambi and P. Pierleoni, "Design of an all-optical wavelength router based on spatial solitons," *J. Lightwave Technol.*, vol. 17, p. 1670, 1999.
17. O. Cohen, T. Carmon, M. Segev and S. Odoulov, "Holographic Solitons," *Opt. Lett.,* vol. 27, p. 2031, 2002.
18. M. J. Ablowitz, G. Giondini, S. Chakravrty, R. B. Jenkins and J. R. Sauer, "Four-wave mixing in wavelength-division-multiplexed soliton systems: ideal fibers," *J. Opt. Soc. Am. B*, vol. 14, p. 1788, 1997.